ORIGINAL SCIENTIFIC PAPER

CROATICA CHEMICA ACTA

Croat. Chem. Acta **2015**, *88*(4), 531–537
Published online: February 20, 2016
DOI: 10.5562/cca2782

HKD 1926

Variable Temperature ^{57}Fe-Mössbauer Spectroscopy Study of Nanoparticle Iron Carbides

Alex Scrimshire,[1,*] Alex L. Lobera,[2] Roman Kultyshev,[3] Peter Ellis,[3] Susan D. Forder,[1] Paul A. Bingham[1]

[1] Materials and Engineering Research Institute, Sheffield Hallam University, City Campus, Howard Street, Sheffield, S1 1WB, UK
[2] Ecole des Mines de Nantes, 4 Rue Alfred Kastler, BP 20722, 44307 Nantes Cedex 3, France
[3] Johnson Matthey Technology Centre, Sonning Common, Reading, West Berkshire, RG4 9NH, UK
* Corresponding author's e-mail address: Alex.Scrimshire@student.shu.ac.uk

RECEIVED: March 15, 2015 * REVISED: July 15, 2015 * ACCEPTED: September 15, 2015

THIS PAPER IS DEDICATED TO DR. SVETOZAR MUSIĆ ON THE OCCASION OF HIS 70TH BIRTHDAY

Abstract: Near-phase-pure nanoparticle iron carbides (Fe_3C and Fe_5C_2) were synthesised. Debye model calculations were used with hyperfine parameters gathered by ^{57}Fe Mössbauer spectroscopy within a temperature range of 10 K to 293 K, with analysis providing Debye temperatures of 422 K and 364 K for two Fe sites in Fe_5C_2 and 355 K for ferromagnetic Fe_3C. The intrinsic isomer shifts were calculated as 0.45 mm s^{-1} and 0.43 mm s^{-1} for iron sites 1 and 2 respectively in Fe_5C_2 and 0.42 mm s^{-1} for Fe_3C. Recoil-free fractions for the two iron sites were also calculated at f_{300} 0.785 and 0.726 for site 1 and 2 respectively.

Keywords: Mössbauer, iron carbides, Debye, Hägg, cementite, catalyst.

INTRODUCTION

IRON carbides have a variety of uses and fields of interest, from their ubiquity in iron and steel manufacturing[1] to super capacitor electrodes[2] and functionalized carbon nanotubes.[3] Iron-based catalysts are widely used in Fischer-Tropsch synthesis (FTS)[4,5] with iron carbides giving high levels of activity and selectivity in producing the desired longer hydrocarbon chains.[6] Characteristics of iron carbides as compounds may vary greatly, as summarized in Table 1.

At present it is believed that the Hägg carbide (χ-Fe_5C_2 as in Table 1) is a highly active iron carbide phase in FTS while cementite, Fe_3C (also called Cohenite), is considered far less active.[4,7] This work is intended to probe the iron environments within nanoparticle cementite and Hägg carbide as inactive and active FTS catalyst iron carbide phases in order to improve the understanding of these potential industrial catalysts. Through an increased understanding, and use of the Debye model to ascertain a Debye temperature for these phases, mixed-phase catalysts that have been in service may be studied to determine any differences in phase abundance to relate their abundance to catalytic activity. Hence the aim is to more confidently identify active FTS iron carbide phases. Nanoparticles are being studied for their greater surface area by weight with the intent to identify any surface phases that would be in direct contact with the reactants. For these phases in low abundances, ^{57}Fe transmission Mössbauer spectroscopy is the ideal technique to study these iron-rich materials. ^{57}Fe Mössbauer spectroscopy uses gamma radiation emitted from a ^{57}Co source to probe the ^{57}Fe nuclei of a sample material, with an energy resolution to the order of 1 in 10^{12},[8] allowing hyperfine interactions around the nuclei to be investigated. Transitions of a material may also be observed using Mössbauer spectroscopy by placing the material in relevant environments for that transition to occur, such as pressure, an external magnetic field or non-ambient temperatures. In this work, the temperature will be controlled with a closed-cycle helium cryogenic system allowing sub-ambient temperatures from 10 to 293 K to be achieved. By investigating a material at a range of temperatures any transitions revealed by spectral changes will allow more

Table 1. Iron carbide phase characteristics[6]

		Formula	Atomic ratio (C : Fe)	Crystal lattice	Interstitial occupation of carbon atoms	Wt% C
Hexagonal carbide	ε	Fe_2C	0.5	hcp to monoclinic	Octahedral	9.7
	ε'	$Fe_{2.2}$	0.45	hcp to monoclinic	Octahedral	8.9
Eckstrom and Adcock carbide		Fe_7C_3	0.43	Orthorhombic	Trigonal prismatic	8.4
Hägg carbide	χ	Fe_5C_2	0.4	Monoclinic	Trigonal prismatic	7.9
Cementite	θ	Fe_3C	0.33	Orthorhombic	Trigonal prismatic	6.7
		Fe_xC				

confident phase identification of mixed phase systems, such as catalysts. This will allow comprehensive aging studies to be carried out, and active phases of a catalyst may be more confidently determined.

METHODOLOGIES

Two near-phase pure sample were synthesised, one of cementite (Fe_3C) and one of Hägg carbide (Fe_5C_2). The cementite was prepared by decomposition of a mixture of iron(III) acetate and gelatin at 700 °C.[9] The nanoparticles of Hägg carbide, Fe_5C_2, were prepared by decomposition of iron pentacarbonyl in the presence of hexadecyltrimethylammonium bromide (CTAB) at 350 °C.[10] The details of the synthesis procedures may be found in the relevant sources provided.

X-ray diffraction was performed on a Bruker AXS D8 with a copper Kα source tube; 2ϑ 10 to 130; step size 0.022°; step time 176 seconds; 25 °C. Analysis of the samples indicated that the cementite samples contained 98 % Fe_3C (04-003-6492) and 2 % Fe metal, and the Fe_5C_2 (00-036-1248) after synthesis indicated largely Fe_5C_2 with traces of cementite and an undefined glassy phase indicated by a broad and tall peak with no defining features. After approximately 20 hours in air, XRD of the Fe_5C_2 sample clearly showed Fe_5C_2, trace amounts of cementite and a potential indication of an iron oxide phase (00-046-1436).

^{57}Fe Mössbauer spectroscopy, with a ^{57}Co in Rh source, was conducted on these samples between 293 and 10 K at a velocity range of ± 12 mm s^{-1} using a See Co W304 and W202 drive unit and 1024 channel spectrometer, with a Janis CCS-800/204N cryostat and Lakeshore 335 temperature controller. Each sample was diluted with fine powder graphite in order to achieve an ideal Mössbauer thickness in the absorber. Data collections above 100 K were conducted under vacuum. For data collections at or below 100 K, the cryostat chamber was filled with helium and maintained at ambient pressure with decreasing temperature. This helium was introduced as an exchange gas having found that temperatures below 100 K were more difficult to maintain under a vacuum, while under helium temperatures of 10 K were easily held. The beginning of each collection was delayed by an hour once the temperature controller stated the desired temperature had been met to ensure the entire chamber was at temperature and to ensure temperature stability.

RESULTS

Each synthesis produced very fine, black, magnetic nanoparticles with XRD identification indicating near phase pure materials. The expected room temperature Mössbauer hyperfine parameters from literature in Tables 2 and 3 present data for nanoparticles and bulk Fe_5C_2 respectively. Uncertainties were not given and where these sources have stated *isomer shift*, this is most likely meaning centre shift, however this has been kept as *IS*.

Experimental values gathered during this study for Fe_5C_2 for the sites most consistent with literature values are presented in Tables 4 and 5 over the temperature range 10 to 293 K. All Mössbauer data from this work is relative to α-Fe calibration.

Figures 1 and 2 show the relation between the experimental values for centre shifts across the temperature range and the expected trends for Debye temperatures of 400 to 600 K, for the two iron sites presented in Tables 4 and 5. As seen in Figure 1, the 100 K data is not consistent with the other experimental centre

Table 2. Nanoparticle Fe_5C_2 Mössbauer parameters[11]

Iron Site	*IS* / mm s^{-1}	*H* / T	*ε* / mm s^{-1}
Site 1	0.288	21.5	0.055
Site 2	0.171	18.16	–0.049

Table 3. Bulk sample Fe_5C_2 Mössbauer parameters[6]

Iron Site	*IS* / mm s^{-1}	*H* / KoE [T]
Site 1	0.46	189 [18.9]
Site 2	0.51	218 [21.8]
Site 3	0.23	216 [21.6]

Table 4. Experimental values of Mössbauer hyperfine parameters for site 1; nanoparticles of Fe_5C_2. *CS*: Centre shift (± 0.02 mm s^{-1}); *H*: Magnetic splitting (± 0.5 T); *Γ*/2 = HWHM (± 0.02 mm s^{-1}); *ε*: Quadrupole shift (± 0.02 mm s^{-1})

T / K	*CS* / mm s^{-1}	*H* / T	(*Γ*/2) / mm s^{-1}	*ε* / mm s^{-1}
293	0.23	21.9	0.19	0.03
250	0.24	22.4	0.18	0.04
200	0.27	23.3	0.18	0.03
150	0.30	24.2	0.18	0.03
147.5	0.30	24.2	0.17	0.03
137.5	0.31	24.3	0.17	0.03
125	0.31	24.5	0.17	0.03
100	0.32	24.6	0.22	0.02
50	0.33	25.2	0.18	0.02
10	0.34	25.4	0.17	0.03

Table 5. Experimental values of Mössbauer hyperfine parameters for site 2; nanoparticles of Fe_5C_2. *CS*: Centre shift (± 0.02 mm s^{-1}); *H*: Magnetic splitting (± 0.5 T); *Γ*/2 = HWHM (± 0.02 mm s^{-1}); *ε*: Quadrupole shift (± 0.02 mm s^{-1})

T / K	*CS* / mm s^{-1}	*H* / T	(*Γ*/2) / mm s^{-1}	*ε* / mm s^{-1}
293	0.21	20.0	0.23	0.01
250	0.22	20.5	0.26	0.01
200	0.26	21.6	0.27	0.02
150	0.29	22.2	0.29	0.00
147.5	0.29	22.3	0.30	0.02
137.5	0.31	22.4	0.32	–0.02
125	0.31	22.4	0.31	0.01
100	0.28	22.0	0.33	–0.01
50	0.32	23.0	0.30	0.02
10	0.33	23.2	0.26	0.02

shift trend, and as such it was omitted from calculations to come.

Figure 3 shows the Mössbauer spectra for 293, 150 and 137.5 K, chosen for the visible additional phase becoming present at 137.5 K at around the ± 8 mm s^{-1} regions. Mössbauer spectra were fitted using Lorentzian model lines with Recoil software. The fitting process allowed centre shift, magnetic splitting, quadrupole shift area and linewidth to vary, while the sextets were constrained to a 3:2:1 ratio regarding the peak height, and the linewidth of paired peaks (1 and 6, 2 and 5, 3 and 4) were kept the same.

Tables 6 and 7 present existing literature data for Fe_3C, all concerning room temperature measurements, uncertainties were not provided by the authors, nor was the calibration material stated; it is assumed to be α-Fe.

There is also reportedly a doublet associated with Fe_3C at 293 K. Table 7 contains the experimental data

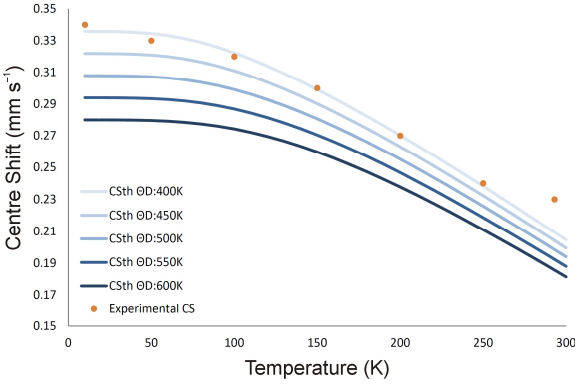

Figure 1. Experimental centre shifts of Fe_5C_2 site 1 against theoretical centre shift trend lines calculated.

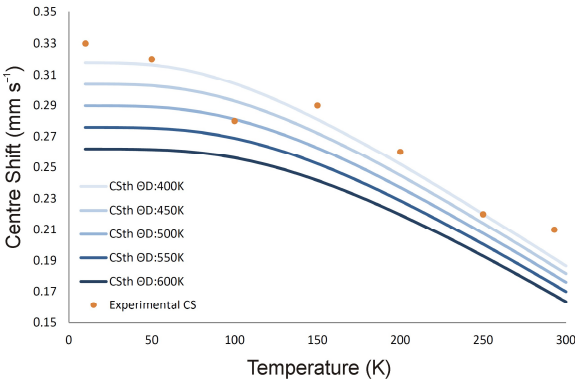

Figure 2. Experimental centre shifts of Fe_5C_2 site 2 against theoretical centre shift trend lines calculated.

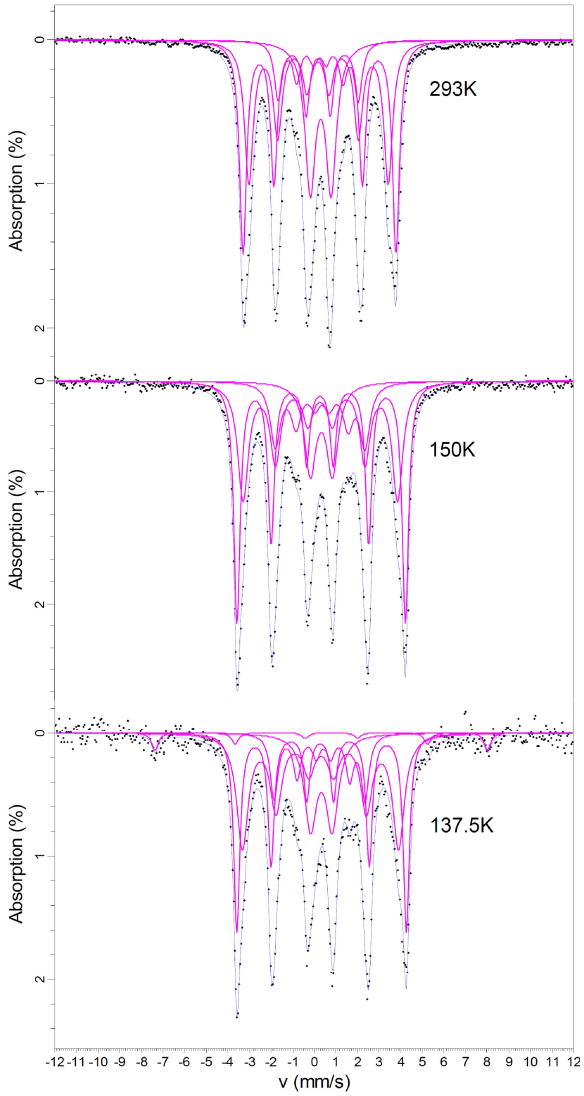

Figure 3. Experimental data and Lorentzian line fits of Fe_5C_2 Mössbauer spectra.

gathered in this work for the corresponding sextet, over a temperature range of 50 to 293 K.

Figure 4 shows the experimental centre shifts with temperature, and the expected trends according to the Debye model. All data points appear to follow the expected trend within the Debye model, and as such all were included and used in further calculations.

Table 6. Nanoparticle ferromagnetic Fe_3C Mössbauer hyperfine parameters[12]

T / K	*CS* / mm s^{-1}	*H* / T	ε / mm s^{-1}
293	0.19	20.5	0.01
60	0.32	24.9	–0.05
27	0.32	25.0	0.01

ANALYSIS AND DISCUSSION

The room temperature hyperfine parameters from literature (Tables 2 and 3) are notwithin the experimental uncertainties for the current experimental values for the two iron sites of Fe_5C_2 in Tables 4 and 5. While the spectrum of Fe_5C_2 at roomtemperature does have more components than the two sextets presented in Cheng,[11] their synthesis route is different to that used for this study, and material synthesisroute is believed to have an effect on hyperfine structure and therefore on the Mössbauer data.[13] The trend seen for both iron sites agree with that expected for the Debye model, as seen in Figures 1 and 2. Within the Debye Model framework,[14] the recoil free fraction parameter can be determined by equation 1:

$$\ln f = -\frac{3E_\gamma^2}{Mc^2}\frac{1}{k\Theta_D}\left[\frac{1}{4}+\left(\frac{T}{\Theta_D}\right)^2\int_0^{\Theta_D/T}\frac{x\mathrm{d}x}{e^x-1}\right] \quad (1)$$

where (in case of ^{57}Fe-Mössbauer study):

E_γ, Energy of the gamma ray = 14.4125 keV (2.30914 × 10^{-15} J),

M, Mass of ^{57}Fe = 9.46507 × 10^{-26} kg,

c, Speed of light = 299 792 458 m s^{-1},

k, Boltzmann constant = 1.38065 × 10^{-23} J K^{-1},

Θ_D, Debye temperature – Sample dependent constant (K),

T, Absolute temperature of the sample – Variable (K)

Table 7. Experimental Mössbauer Parameters of Fe_3C, *CS* Relative to α-Iron. *CS*: Centre shift (± 0.02 mm s^{-1}); *H*: Magnetic splitting (+/- 0.5 T); $\Gamma/2$ = HWHM (± 0.02 mm s^{-1}); ε: Quadrupole shift (± 0.02 mm s^{-1})

T / K	*CS* / mm s^{-1}	*H* / T	(Γ/2) /mm s^{-1}	ε / mm s^{-1}
293	0.19	20.8	0.19	0.01
250	0.22	22.0	0.20	0.01
200	0.25	23.1	0.21	0.00
150	0.28	23.9	0.20	0.00
100	0.31	24.6	0.2	0.00
55	0.32	24.9	0.21	–0.01
50	0.32	25.0	0.19	0.00

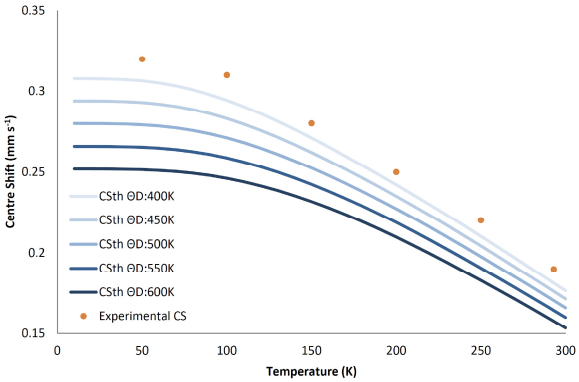

Figure 4. Experimental centre shifts of Fe_3C against theoretical centre shift trend lines calculated.

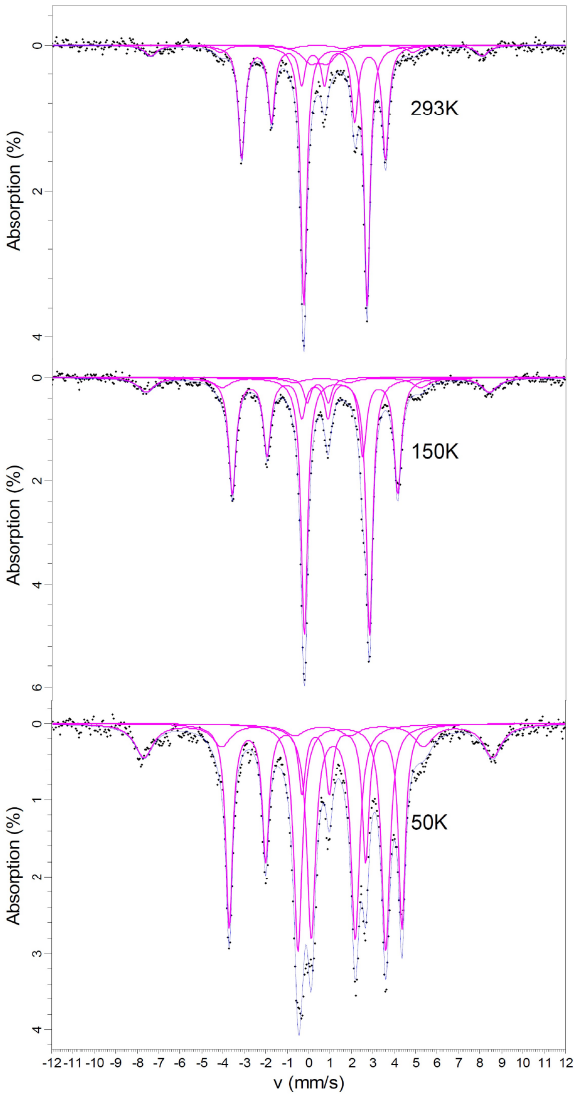

Figure 5. Experimental data of Fe_3C Mössbauer spectra with Lorentzian line fits.

The Debye Temperature Θ_D is required to find the recoil free fraction f.

Equation 2 shows the Second Order Doppler effect (SOD) as a function of the Temperature T and the Debye temperature Θ_D:

$$SOD\left(m/s\right) = -\frac{3}{2}\frac{k\Theta_D}{Mc}\left[\frac{3}{8} + 3\left(\frac{T}{\Theta_D}\right)^4 \int_0^{\Theta_D/T} \frac{x^3 dx}{e^x - 1}\right] \quad (2)$$

Equation 3 links the Second Order Doppler effect (SOD) to the Centre Shift(CS):

$$CS_{(T,\Theta_D)} = IS + SOD_{(T,\Theta_D)} \quad (3)$$

where IS, the Isomer Shift, which is considered to be independent of the temperature. By setting these equations as spreadsheet functions the Debye temperature can be calculated. At a given temperature the spreadsheet solver function will vary the Debye Temperature Θ_D and the isomer shift, calculate a theoretical centre shift CS_{th} by means of equations 2 and 3 and compare it with the experimental one CS_{exp}. Let:

$$\Delta\left(\Theta_D, IS, T\right) = \left|CS_{th(\Theta_D, IS, T)} - CS_{exp(T)}\right| \quad (4)$$

Function 4 shows the absolute value of the difference between the theoretical value of centre shift (at given Debye Temperature, isomer shift and temperature) and the experimental one (at given temperature).

By varying the Debye Temperature Θ_D and the isomer shift step by step, the solver will try to minimize the sum $\Sigma_{(\Theta D, IS)}$ of deltas $\Delta(\Theta_D, IS, T)$ corresponding to all the temperatures experimentally analysed:

$$\Sigma\left(\Theta_D, IS\right) = \Delta\left(\Theta_D, IS, 293\,\mathrm{K}\right) + \ldots + \Delta\left(\Theta_D, IS, 10\,\mathrm{K}\right) \quad (5)$$

The Debye Temperature and isomer shift being calculated can be set with constrictions, such that the initial calculation is run with wide allowances, before the values are constricted, with larger numbers of iterations with smaller allowable windows. Once $\Sigma(\Theta_D, IS)$ is minimized, the Debye Temperature Θ_D and the isomer shift IS are known. Then, it becomes possible to calculate the recoil free fraction f by means of equation 1. By manipulating these equations for set Debye Temperatures, the trend lines in Figures 1 and 2 were plotted for comparison with the experimental centre shifts gathered in this study, allowing

an estimate of the actual Debye temperature to be made and used as a limiting parameter for the solver function.

By utilising these Debye model equations with the experimental data gathered, the Debye Temperature of Fe_5C_2 iron site 1 was determined as 422 K, and site 2 as 364 K. The intrinsic isomer shifts were calculated as 0.45 mm s^{-1} and 0.43 mm s^{-1} (± 0.03 mm s^{-1}) for iron sites 1 and 2 respectively. These were calculated by omitting the 100 K and 293 K data as these did not agree with the trends expected in the Debye model, the reason for this being currently unknown. Although experimental error may allow these values to have been used, with the current functions being used in the spreadsheet formula, it is necessary that decreases in temperatures is accompanied by increases in centre shift, or else the function is not satisfied and errors are returned. The sum of the magnitude of differences between the theoretical and experimental centre shifts as presented in equation 5 was 0.03 without the 100 K and 293 K data, which may be considered the uncertainty of the intrinsic isomer shifts stated.

The Fe_3C data from Table 7 was also processed using the Debye model calculation spreadsheet, yielding an intrinsic isomer shift of 0.42 mm s^{-1} (± 0.03 mm s^{-1}) and a Debye temperature of 355 K. The magnitude of the differences between the theoretical and experimental data was 0.03, which may again be considered the uncertainty. Data from Fe_3C collected below 55 K was not included in this work, due to the spectral change seen in the 50 K spectrum of Figure 5. The nature of this spectral change is not currently known, but can be seen in the 2009 work by David *et al*.[12]

For comparison of Debye temperatures, it appears that different methods of calculation, and the experimental approach used has profound effects on the outcome, as summarised in Table 8 for Fe_3C.

As such, the values stated in this work are for consideration of Mössbauer data, and the mathematical approach using the Debye model as detailed. This wide range of existing values may be due to the nature in which the Fe_3C is being studied, while that studied in this work is ex situ as nanoparticles. A combination of the approaches used by each author, the particle size and surrounding matrix of the cementite may give rise to these great variances in reported values.

The difference between Debye temperatures of the two identified iron sites within Fe_5C_2 indicates that the iron in site 1 is held more tightly than the iron in site 2. A higher Debye temperature gives a higher recoil-free fraction, and site 1 will contribute more to the Mössbauer spectrum than the same amount of iron in site 2. Through the execution of equation 1 within our program we can calculate the recoil free fractions for both site 1 and site 2 as f_{300} 0.785 and 0.726, respectively. The greater recoil-free fraction would agree with the greater Debye temperatures calculated for the two iron sites in Fe_5C_2, both caused by site 1 being more tightly bound and therefore less able to vibrate than iron site 2.

Table 8. Summary of published Debye temperatures for Fe_3C by author

Source	Fe_3C Debye Temperature Reported (K)
This work	355 (± 25)
Ledbetter[15]	501 (± 27)
Wood[16]	604 (± 44)
Guillermet and Grimvall[17]	394

The hyperfine parameters gathered through this study, and the Debye temperature and recoil-free fraction that can be calculated can be used to confidently identify mixed iron carbide materials, such as catalysts after having been in service, to enable aging studies. By having reference data to refer to for mixed phase samples, any phases that may evolve through catalytic activity can be identified to better understand the nature of the catalysis.

CONCLUSIONS

Through the use of Debye model equations, Debye temperatures for nanoparticle iron carbides were calculated using variable temperature ^{57}Fe Mössbauer spectroscopy hyperfine parameter data. Intrinsic isomer shifts of Fe_5C_2 and Fe_3C were proposed by using this method, all of which may aid in better understanding these carbide phases, and mixed phase systems that contain one or both of those studied.

REFERENCES

[1] G. Marest, A. Fontes, J. Roigt, A. Faussemagne, S. Fayeulle, M. Jeandin, A. Benyagoub, N. Moncoffre, M. Frainais, *Hyperfine Interact*. **1995**, *95*, 227.

[2] M. Yan, Y. Yao, J. Wen, W. Fu, L. Long, M. Wang, X. Liao, G. Yin, Z. Huang, X. Chen, *J. Alloy. Compd*. **2015**, *641*, 170.

[3] Q. Su, G. Zhong, J. Li, G. Du, B. Xu, *Appl. Phys. A-Mater*. **2012**, *106*, 59.

[4] J. W. Niemantsverdriet, A. M. Van der Kraan, W. L. Van Dijk, H. S. Van der Baan, *J. Phys. Chem*. **1980**, *84*, 3363.

[5] G. Le Caer, J. M. Dubois, M. Pijolat, V. Perrichon, P. Bussiere, *J. Phys. Chem*. **1982**, *86*, 4799.

[6] E. de Smit, B. M. Weckhuysen, *Chem. Soc. Rev*. **2008**, *37*, 2758.

[7] V. P. Santos, T. A. Wezendonk, J. J. D. Jaén, A. I. Dugulan, M. A. Nasalevich, H.-U. Islam, A. Chojecki,

S. Sartipi, X. Sun, A. A. Hakeem, A. C. J. Koeken, M. Ruitenbeek, T. Davidian, G. R. Meima, G. Sankar, F. Kapteijn, M. Makkee, J. Gascon, *Nature Communications*, **2015**, *6*, 6451.

[8] F. Berry, D. Dickson, *Mössbauer Spectroscopy,* Cambride University Press, **2005**. ISBN 0-521-01810-2.

[9] Z. Schnepp, S. C. Wimbush, M. Antonietti, C. Giordano, *Chem. Mater*. **2010**, *22*, 5340.

[10] C. Yang, H. Zhao, Y. Hou, D. Ma, *J. Am. Chem. Soc*. **2012**, *134*, 15814.

[11] K. Cheng, M. Virginie, V. V. Ordomsky, C. Cordier, P. A. Chernavskii, M. I. Ivantsov, S. Paul, Y. Wang, A. Y. Khodakov, *J. Catal*. **2015**, *328*, 139.

[12] B. David, O. Schneeweiss, F. Dumitrache, C. Fleaca, R. Alexandrescu, I. Morjan, *J. Phys. Conf. Ser*. **2010**, *217*, 012097.

[13] B. Hannoyer, A. A. M. Prince, M. Jean, R. S. Liu, G. X. Wang, *Hyperfine Interact*. **2006**, *167*, 767.

[14] J. J. Quinn, K.-S. Yi, Debye Model. *Solid State Physics, Principles and Modern Applications,* Springer, **2009**.

[15] H. Ledbetter, *Mater. Sci. Eng. A*, **2010**, *527*, 2657.

[16] B. J. Wood, *Earth Planet. Sci. Lett*. **1993**, *117*, 593.

[17] A. F. Guillermet, G. Grimvall, *J. Phys. Chem. Solids*, **1992**, *53*, 105.